

Evolution of the WZ Sge accretion disk throughout quiescence

Paula Kvist,^{a,*} Vitaly Neustroev^a and Valery Suleimanov^b

^a*Space Physics and Astronomy research unit, PO Box 3000, FI-90014 University of Oulu, Finland*

^b*Institut für Astronomie und Astrophysik, Universität Tübingen, Sand 1, D-72076 Tübingen, Germany*

E-mail: paula.kvist@oulu.fi

Properties of accretion disks remain poorly understood in low mass-transfer rate systems such as WZ Sge-type dwarf novae. In particular, the long recurrence intervals from years to decades are challenging to explain. WZ Sge, the prototype of WZ Sge-type dwarf novae, is expected to undergo a superoutburst in the near future. To investigate its state before the outburst, we observed it in 2024 with the Nordic Optical Telescope and in 2025 with X-Shooter of ESO/VLT. We compare these new data with archival data from the current quiescent period to trace the spectral evolution during quiescence. We found a stable continuum with remarkably evolving emission lines throughout the first decade after the previous superoutburst. Furthermore, we estimate the physical parameters of the accretion disk using a two-component hydrogen slab model.

*87th Fujihara Seminar: The 50th Anniversary Workshop of the Disk Instability Model in Compact Binary Stars (DIM50TH2025)
22-26 September 2025
Tomakomai, Japan*

*Speaker

© Copyright owned by the author(s) under the terms of the Creative Commons Attribution-NonCommercial-NoDerivatives 4.0 International License (CC BY-NC-ND 4.0). All rights for text and data mining, AI training, and similar technologies for commercial purposes, are reserved. ISSN 1824-8039. Published by SISSA Medialab.

<https://pos.sissa.it/>

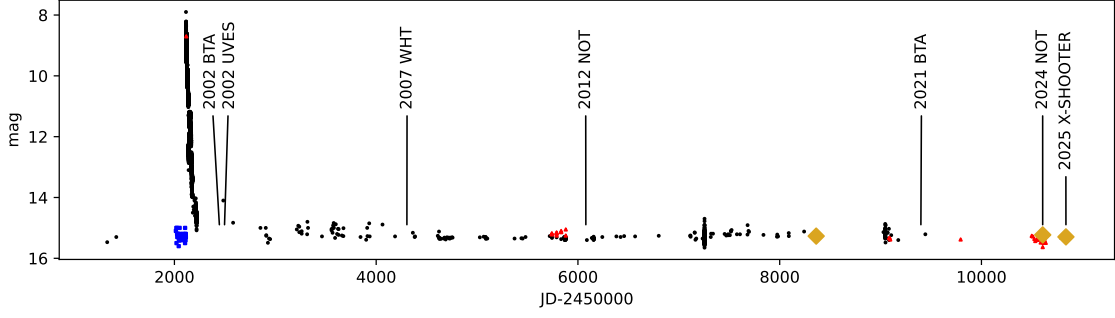


Figure 1: Combined light curve of WZ Sge since its last outburst in 2001. AAVSO V-band magnitudes are in black; AAVSO Visual magnitudes in blue; BAVSS V-magnitude in red; and our own observations (NOT V-band and X-shooter g-band) are in yellow diamonds. The spectroscopic observations, described in more detail in Section 2, are annotated.

1. Introduction

Dwarf novae (DNe) are a type of cataclysmic variables (CVs), interacting binaries with a white dwarf (WD) primary and a low mass donor. In non-magnetic DNe, the mass is accreted from the donor through an accretion disk formed around the WD. From time to time, they undergo outbursts, sudden bursts of accretion, which can brighten the system by 2-5 magnitudes in normal outbursts, and even more in more powerful but rarer superoutbursts.

The outburst behaviour of CVs is described by the Disk Instability Model (DIM) [1–3]. It explains normal outbursts by a thermal instability in the accretion disk, and superoutbursts by a combination of thermal and tidal instabilities. However, the DIM still has problems explaining the outburst properties of a subclass of DNe called WZ Sge-stars. They are evolved CVs with short orbital periods $\lesssim 120$ min, have extremely low mass-transfer rate less than a few $\times 10^{-13} M_{\odot} \text{yr}^{-1}$ [4], and experience only superoutbursts with intervals of years to decades [5].

The DIM can explain the long recurrence intervals with either an extremely low disk viscosity ($\alpha < 0.0001$) or, alternatively, a truncated the inner accretion disk [3]. In the latter case, an enhancement of the mass transfer rate prior to an outburst is also required. Additionally, recent observations of WZ Sge-type objects indicate that the disk remains optically thin until the beginning of a superoutburst [4, 6], when the DIM predicts the mass-transfer rate to rise before an outburst, and the disk to become optically thick in the continuum before an outburst. In order to understand the outburst onset, we need to first understand the physical properties and geometry of accretion disks in low mass-transfer systems in quiescence.

WZ Sge, archetype of the WZ Sge-type objects, is one of the most famous and well-studied dwarf novae. WZ Sge has recorded superoutbursts in 1913, 1946, 1978, and 2001, with outburst intervals of 33, 32, and 23 years. If the next outburst follows the shorter interval, we could expect it to go into an outburst soon. Thus, we observed WZ Sge twice during 2024-2025 and compared our observations with archival data taken during the current quiescent stage. We present the spectral evolution of WZ Sge during the quiescent period from its 2001 outburst until 2025. In addition, we show the state of the accretion disk and estimate its physical properties as observed in 2025.

2. Observations

The analysis of this work is based on spectra of WZ Sge as observed by us in 2025 with the Very Large Telescope (VLT) of the European Southern Observatory (ESO) at the Paranal Observatory in Chile, using the medium-resolution echelle spectrograph X-Shooter. Additionally, we observed WZ Sge in 2024 with the Nordic Optical Telescope (NOT), located in Roque de los Muchachos Observatory (ORM), using the Alhambra Faint Object Spectrograph and Camera (ALFOSC). With the NOT, we obtained both spectroscopic and multicolor photometric data.

We used complementary archival data for the study of spectral evolution. WZ Sge was observed with the VLT using Ultraviolet and Visual Echelle Spectrograph (UVES) in 2002, Bolshoi Teleskop Alt-azimutalnyi (BTA; located in the Northern Caucasus) using UAGS spectrograph in 2002 and SCORPIO-1 in 2021, NOT/ALFOSC in 2012, and William Herschel Telescope (WHT; at the ORM) using Intermediate-dispersion Spectrograph and Imaging System (ISIS) in 2007.

All spectra have been corrected for barycentric velocity. Data taken with ESO instruments have been retrieved from the ESO Science Archive Facility and reduced using default pipelines (UVES Workflow For Point Source Echelle Data version 6.1.6, and X-shooter Workflow for Physical Mode Data Reduction version 3.5.0), within ESO REFLEX version 2.11.5 [7]. Telluric absorption in X-shooter data was corrected using MOLECFIT [8]. Data taken with BTA, NOT, and WHT instruments were retrieved from their respective archives and reduced following basic spectroscopic reduction steps with NOIRLab IRAF version 2.18 [9–11].

3. Photometry

Figure 1 shows the photometric evolution of WZ Sge from the onset of the 2001 superoutburst until this year, together with the timing of the spectroscopic observations. The light curve shows a photometrically stable system for the last two decades. The quiescent brightness is $V \sim 15.2$ mag.

4. Spectral features

Figure 2 shows the orbit-averaged spectrum of WZ Sge, as observed with X-shooter in 2025. The spectrum is dominated by spectral lines of hydrogen and helium. The WD is visible in wide Balmer absorption lines in the blue part of the spectrum. Double-peaked Balmer emission lines, originating from the accretion disk, are visible up to H15. Hydrogen emission is also visible in the Paschen (up to P13) and Brackett (up to Br14) series.

Additionally we see emission in He I (4471, 4921, 5015, 5876, 6678, 7065, 10830 Å), He II (4685.682 Å), Ca II (3934 Å; triplet 8498+8542+8662 Å), O I (7774, 8446 Å), and lines of iron, e.g. Fe II (5169 Å). From trailed spectra, one can see that these lines are associated with the hot spot (see also [6]).

Due to the excellent spectral resolution provided by X-shooter, we detect the faint donor star in several spectral lines. It is best visible in the Si I 3905 Å emission and K I 12522 Å absorption lines. An additional absorption line from the donor, likely Fe I, is found around 15022 Å.

We note that the X-shooter spectrum has the widest wavelength coverage in all available data. The NIR end of the spectrum has the best S/N observed so far, enabling us to see previously

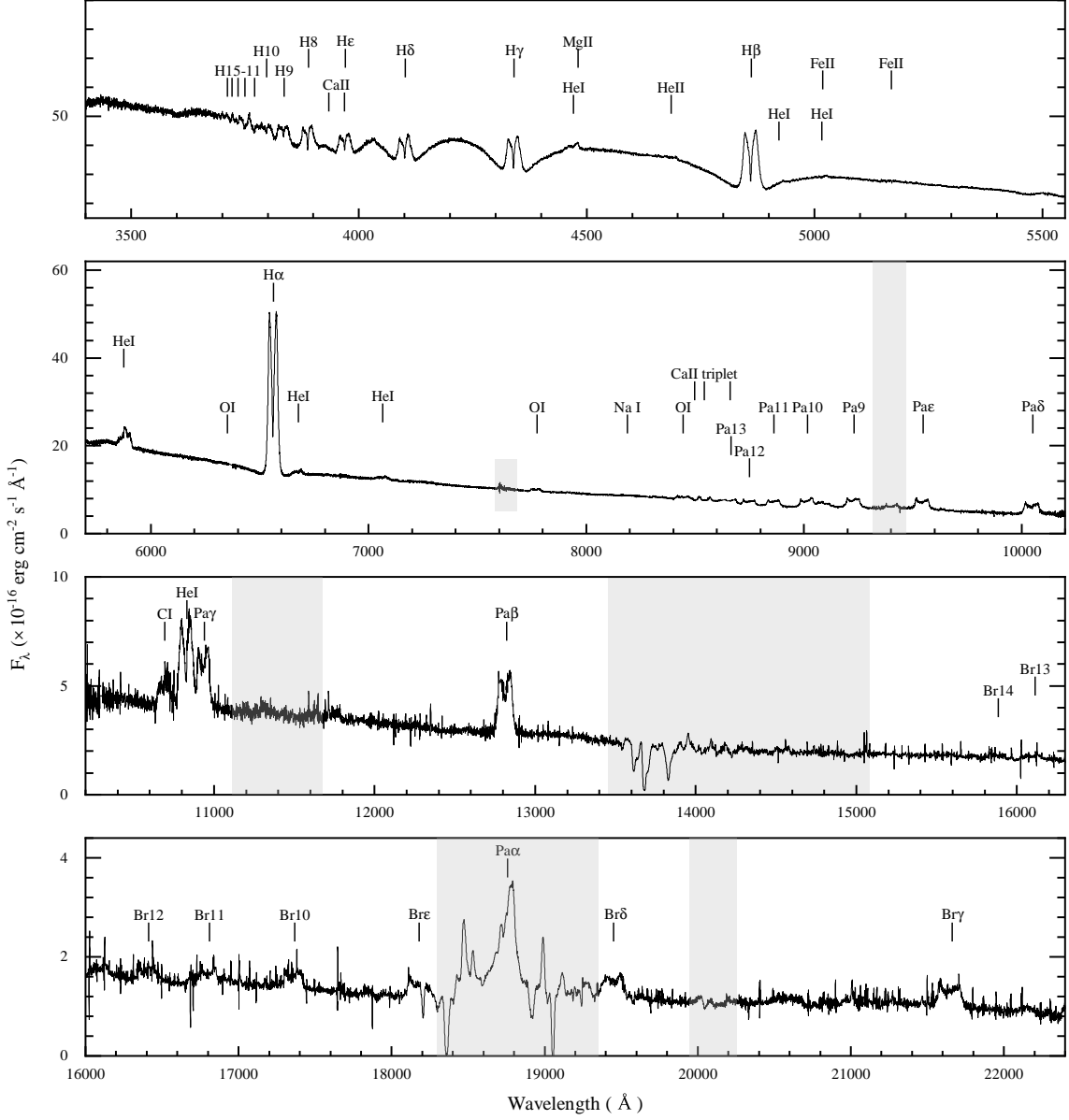


Figure 2: The average spectrum of WZ Sge as obtained with X-Shooter in June 2025, with the most prominent lines labelled. The telluric absorption bands are highlighted in grey.

unobserved features. While this work is focused on the optical and UVB data, our future work will focus on the traces of the donor in the NIR spectrum.

4.1 Emission line evolution in quiescence

Figure 3 shows the evolution of the H β and H γ lines from 2002 until 2025. The emission lines strengthen steadily until about 2007, indicating that the disk continued to evolve for several years after the outburst. Spectra in years 2007 and 2012 show a reversed trend, and the lines gradually weaken. By 2021, the disk appears to have reached an equilibrium state, with no remarkable changes in the emission lines to this day.

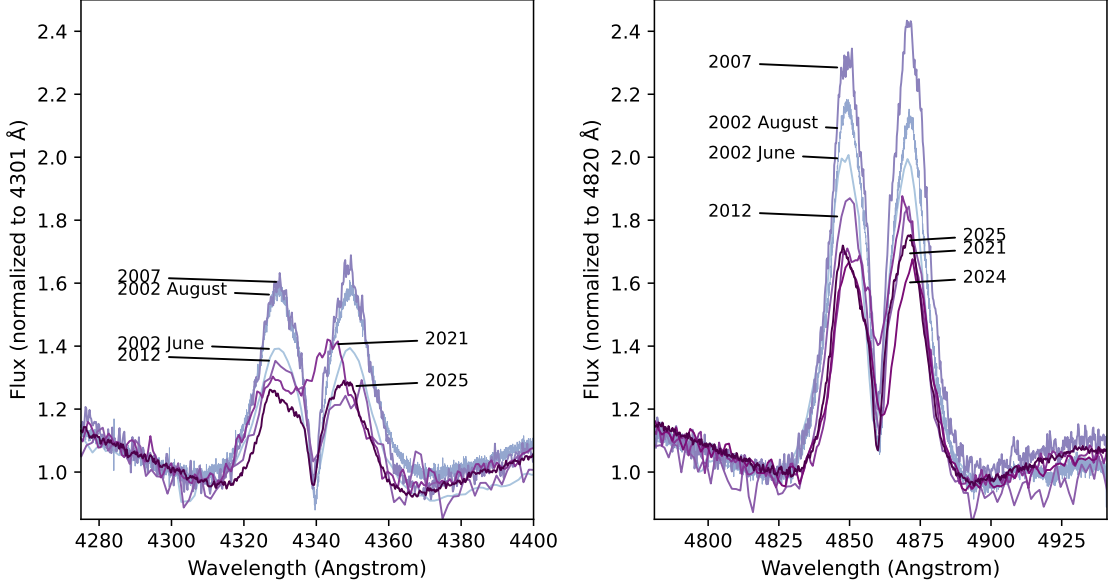


Figure 3: Temporal evolution of the H_γ (left) and H_β (right) emission lines. Initially, after the 2001 outburst, the spectral lines strengthened up to 6 years post-outburst, after which they started to weaken gradually. The emission lines have been stable since at least 2021. The H_γ emission line returns to quiescent levels faster than H_β .

We suspect that the evolution of the line intensity can be used to gauge the accretion disk properties at different stages. The emission processes are different for the formation of the continuum and the formation of emission lines. The most dominant lines, the Balmer and Paschen series, are formed via recombination when free electrons are captured into excited hydrogen states and subsequently cascade to lower levels, releasing photons. Strong line emission requires a high fraction of ionized hydrogen, temperatures low enough to permit recombination, and an adequate particle density. The optical continuum, on the other hand, is primarily determined by the gas temperature and pressure. The changes in continuum levels throughout the quiescence are minimal, and thus variations in the ionization fraction are expected to be the dominant factor governing the strength of the emission lines. However, further work is required in this area.

5. Physical properties of the accretion disk

The total observed spectrum is a combination of emission and absorption from the WD, accretion disk, hot spot, and the donor star. We first fit the observed spectrum with a WD + blackbody accretion disk (see [4]) with known WD mass $M_{WD} = 0.8 M_\odot$ [14] and WD temperature 13 750 K and then removed this model atmosphere from the total spectrum, resulting in a spectrum of the accretion disk, hot spot, and the donor. The donor is too faint in visual and UVB wavelengths to have any significant contribution, and thus, we ignore it in our following fitting procedure.

We modeled the optical continuum and Balmer emission of the leftover spectrum using a hydrogen slab model, commonly adopted for approximating accretion disk spectra [12, 13, 15], with previously mentioned WD mass and known inclination angle 75.89° [16]. The model has

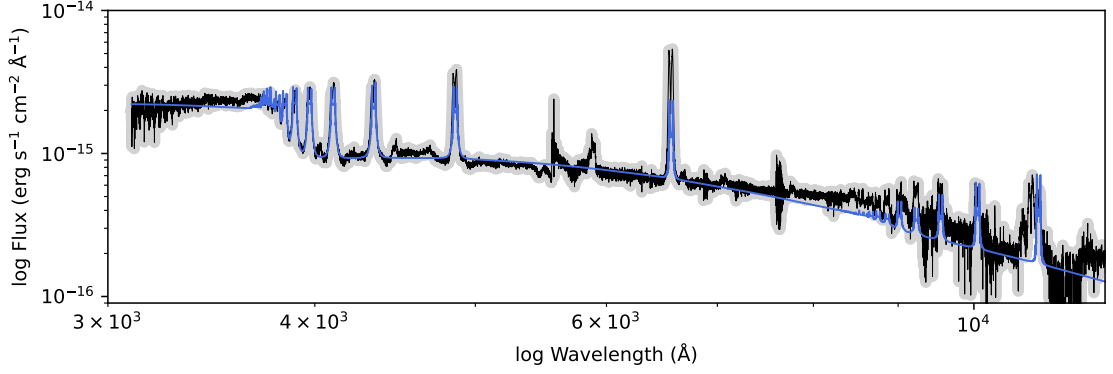


Figure 4: Orbit-averaged spectrum of WZ Sge with the WD contribution removed (black with grey background), together with a two-component hydrogen slab model (blue).

five free parameters: the inner and outer disk radius, temperature, pressure, and disk height. The accretion disk is modeled as a homogeneous, isobaric and isothermal disk around the WD, with constant disk height from R_{in} to R_{out} . The location of the hot spot is not derived from a specific physical prescription, but implemented as a narrow ring at an arbitrary radius, as its precise location does not affect the spectral shape significantly.

We were not able to reproduce the spectral shape with a single-component model at all, implying that the hot spot must be considered when trying to accurately model dwarf nova spectra. Thus, we used a model comprised of two components: the hot spot and the accretion disk. Our fitting procedure was as follows:

1. A model spectrum is calculated with approximate accretion disk parameters.
2. A model spectrum is calculated with approximate hot spot parameters.
3. We combine the two model spectra, each with a respective contribution factor, and convolve it with an instrumental profile matching with X-shooter resolution.
4. The model spectrum is compared with the observed spectrum, and χ^2 -statistic is calculated for the fit.
5. The initial model parameters are modified for either accretion disk model or hot spot model, and the process is repeated until we find a satisfactory fit at a local χ^2 -minimum.

The fitting procedure does struggle with degeneracy, as there are multiple local minima for simple χ^2 -statistic. To solve this, we also take into account the general spectral shape, especially the shape of the Balmer jump, the continuum between 4000 – 7000 Å, and the Balmer line strengths, permitting us to exclude any local minima that do not actually replicate the observed spectrum.

The best-fit parameters of the combined model are listed in Table 1. Considering ideal gas, these conditions would lead to a surface density of $\sim 0.03 \text{ g/cm}^2$. Similarly small value for surface density is obtained through the Balmer decrement and the equivalent width of emission lines [4]. We note that it is possible to get a similar spectral shape with moderately differing parameters, and further work will be needed to improve the fitting procedure.

Table 1: Set parameters for the two-component model, producing the spectra seen in Figure 4

component	T (K)	P (dyn/cm ²)	z (cm)	R _{in} (cm)	R _{out} (cm)
hot spot	10 000	3300	10 ⁷	1.6 × 10 ¹⁰	1.7 × 10 ¹⁰
accretion disk	5 400	150	10 ⁸	7.7 × 10 ⁸	2.0 × 10 ¹⁰

6. Conclusions

1. A two-component hydrogen slab model provides significantly improved spectral modelling in low mass-transfer rate systems such as WZ Sge-type DNe, compared to a single-component model.
2. We find that now, 24 years after the previous superoutburst, the accretion disk in WZ Sge has a very low luminosity $L_d \approx 1.6 \times 10^{30} \text{ erg s}^{-1}$, indicating a very low mass accretion rate $\dot{M}_{acc} \approx 1.0 \times 10^{13} \text{ g s}^{-1} \approx 1.6 \times 10^{-13} M_{\odot} \text{ yr}^{-1}$ and mass-transfer rate $\dot{M}_{tr} \approx 2.4 \times 10^{14} \text{ g s}^{-1} \approx 3.8 \times 10^{-12} M_{\odot} \text{ yr}^{-1}$ (see [4] for details). There is no evidence of the accretion disk of WZ Sge becoming optically thick in June 2025.
3. If WZ Sge were to follow the shorter cycle and outburst soon, the trigger cannot be explained by DIM.

7. Acknowledgements

We are grateful to the Fujihara Foundation of Science for providing financial support that enabled us to attend this workshop.

Based on observations collected at the European Organisation for Astronomical Research in the Southern Hemisphere under ESO programme(s) 115.288W.001 and 69.D-0391(A).

The data presented here were obtained in part with ALFOSC, which is provided by the Instituto de Astrofísica de Andalucía (IAA) under a joint agreement with the University of Copenhagen and NOT.

The William Herschel Telescope is operated on the island of La Palma by the Isaac Newton Group of Telescopes in the Spanish Observatorio del Roque de los Muchachos of the Instituto de Astrofísica de Canarias.

Observations with the SAO RAS telescopes are supported by the Ministry of Science and Higher Education of the Russian Federation. The renovation of telescope equipment is currently provided within the national project "Science and Universities".

NOIRLab IRAF is distributed by the Community Science and Data Center at NSF NOIRLab, which is managed by the Association of Universities for Research in Astronomy (AURA) under a cooperative agreement with the U.S. National Science Foundation.

We acknowledge funding to support the scientific use of our ESO data from the Finnish Centre for Astronomy with ESO (FINCA), University of Turku, Finland.

VS thanks the German Research Foundation (DFG) grant WE 1312/59-1 for financial support.

References

- [1] Osaki, Y. 1974, PASJ, 26, 4, 429. doi:10.1093/pasj/26.4.429
- [2] Lasota, J.-P. 2001, New A Rev., 45, 7, 449. doi:10.1016/S1387-6473(01)00112-9
- [3] Hameury, J. M. 2020, Advances in Space Research, 66, 5, 1004. doi:10.1016/j.asr.2019.10.022
- [4] Neustroev V. V. , Kvist, P., Siitonen, M. and Vuolteenaho, V. 2026, 87th Fujihara Seminar: The 50th Anniversary Workshop of the Disk Instability Model in Compact Binary Stars 016.
- [5] Kato, T. 2015, PASJ, 67, 6, 108. doi:10.1093/pasj/psv077
- [6] Neustroev, V. V. & Mäntynen, I. 2023, MNRAS, 523, 4, 6114. doi:10.1093/mnras/stad1730
- [7] Freudling, W., Romaniello, M., Bramich, D. M., et al. 2013, A&A, 559, A96. doi:10.1051/0004-6361/201322494
- [8] Kausch, W., Noll, S., Smette, A., et al. 2015, A&A, 576, A78. doi:10.1051/0004-6361/201423909
- [9] Tody, D. 1986, Proc. SPIE, 627, 733. doi:10.1117/12.968154
- [10] Tody, D. 1993, Astronomical Data Analysis Software and Systems II, 52, 173.
- [11] Fitzpatrick, M., Placco, V., Bolton, A., et al. 2025, Astronomical Data Analysis Software and Systems XXXIII, 541, 461. doi:10.26624/CETF5821
- [12] Gänsicke, B. T., Beuermann, K., & Thomas, H.-C. 1997, MNRAS, 289, 2, 388. doi:10.1093/mnras/289.2.388
- [13] Hernández Santisteban, J. V., Echevarría, J., Zharikov, S., et al. 2019, MNRAS, 486, 2, 2631. doi:10.1093/mnras/stz798
- [14] Pala, A. F., Gänsicke, B. T., Belloni, D., et al. 2022, MNRAS, 510, 4, 6110. doi:10.1093/mnras/stab3449
- [15] Pala, A. F., Schmidtobreick, L., Tappert, C., et al. 2018, MNRAS, 481, 2, 2523. doi:10.1093/mnras/sty2434
- [16] Skidmore, W., Wynn, G. A., Leach, R., et al. 2002, MNRAS, 336, 4, 1223. doi:10.1046/j.1365-8711.2002.05857.x